A New High Gain Quadratic DC-DC Boost Converter for Photovoltaic Applications

1st Zainab A. Ghafour
Department of Electrical power Engineering Techniques
Middle Technical University
Electrical Engineering Technical College
Baghdad, Iraq
eng.zainab777@gmail.com

2nd Ahmed R. Ajel
Department of Electrical power Engineering Techniques
Middle Technical University
Electrical Engineering Technical College
Baghdad, Iraq
dr_ahmed.R@mtu.edu.iq

3rd Naseer M. Yasin
Department of Electrical power Engineering Techniques
Middle Technical University
Electrical Engineering Technical College
Baghdad, Iraq
naseeryasin@yahoo.com

***Abstract*— This research describes a new configuration for the step-up DC-DC converter. Distributed generation (DG) components such as solar PV arrays, micro-turbines fuel cells, and ultra-capacitors are part of a DC micro-grid; the output voltage in DC micro-grids heavily relies on the DC-DC converter. Increasing the output voltage of a DC-DC converter is required due to the low output voltage of DG sources. Since the voltage stress would be a significant drawback of conventional boost converters, this suggested configuration was designed with quadratic voltage gain and lower voltage stress which reduced the voltage stress across the switch. Structure we compared our configuration with the different designs like positive super lift Luo throughout the paper. The validation of theoretical findings demonstrates simulation and experimental results.**

***Keywords*— new step-up boost converter, quadratic boost converter (QBC), PV system, high DC gain ratio.**

I. Introduction

In recent years, DC-DC converters have played an integral role in renewable energy power systems. The DC-DC converter assists the maximum power point tracking (MPPT) reach the whole PowerPoint and keeps the DC-link constant [1]. Also, the function of a transducer is to process and control the flow of electrical energy by providing voltages and currents that are best suited to the user's loads. Generally, DC/DC converters are labeled into isolated and non-isolated power converters classes. Boost, Buck-Boost, Cuk, and SEPIC converters are Non-isolated (DC-DC) converters characterized by inexpensive, tiny, low switching losses and are more efficient. DC-DC converts DC power from one voltage level to another. Modern electronic power systems demand a power source with high reliability, efficiency, and less input ripple [2, 3]. Parasitic components limit the voltage and efficiency of all DC-DC converters. The LUO converter is a DC-DC converter developed from a boost converter to overcome the aforementioned effects. LUO converters power several technologies to improve the voltage, such as Voltage Lift (VL) and Super lift (SL) technology. The positive output super-lift LUO (POSL) converter is the most commonly used in the Luo converters family; the family types include elementary, re–lift, and triple circuits [4-6]. Several researchers have addressed the low voltage gain in DC-DC converters by adding components to the elementary circuit; many ways have been developed to increase profit while lowering costs and increasing efficiency [7-11]. The authors presented an enhanced DC-DC Boost converter in PV applications [12]. The usage of single-switch and switched inductors to design a high-gain DC-DC converter [13]. The Modified quadratic boost base converters of several types are suggested, which have disadvantages such as low voltage gain ratio and high ripple input current [14, 15].

This paper proposes a new quadratic converter configuration to produce a high DC gain ratio to boost the low voltage from the PV system or any other clean sources. Single switch control would be important of the new converter. Furthermore, one circuit control controlled our suggested converter which is designed in a continuous condition mode (CCM).

II. Proposed new configuration step-up DC-DC converter

The traditional boost converter is shown in “Fig. (1. a)”, voltage gain (G) of the conventional converter as indicated in the “equation (1)”, “Fig. (1. b)” depicts the proposed new converter. The new proposed converter consists of two inductors (L1, L2), four diodes (D1, D2, D3, Do), three capacitors (C1, C2, Co), and one switching (S). The new converter has a higher gain ratio with a simple structure than the literature review mentioned in the introduction section. The analysis of the proposed converter is described in the below sections.

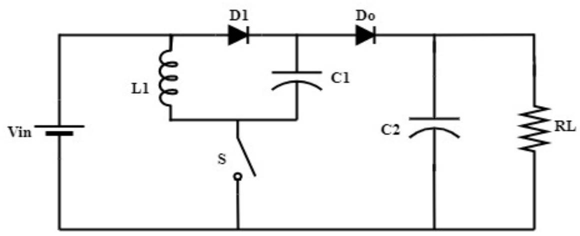

Fig.1. a. The elementary circuit of (POSL) converter [4].

The transfer ratio of voltage (G) of the elementary (POSL) converter as follows:

$$G = \frac{V_O}{V_{in}} = \frac{2-D}{1-D} \quad (1)$$

D: is the duty cycle of the power switch.

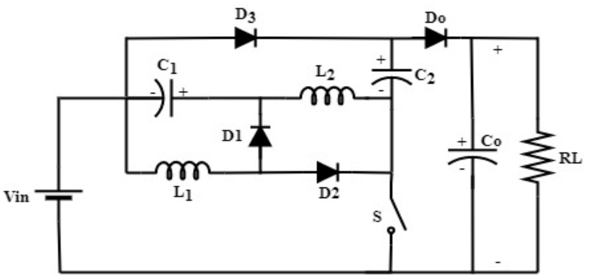

Fig. 1.b. Circuit configuration of a proposed new converter

A. *The analysis of the new proposed configuration.*

The Proposed Converter's structure is shown in "Fig. (1.b)"; the principle of the converter is to charge the passive element during the switch and discharge the energy during the off switch depending on the control signal. The operation has two switch mode ON and OFF as shown in "Fig. (2.a)" and "Fig. (2.b)". In this paper, the analysis equations are driving in continuous conduction mode (CCM). The operational modes can be explained as follows:

Mode 1: during the switch (S) is turned ON, the first inductor (L1) and capacitor (C2) are charged in parallel while the capacitor (C1) and inductor (L2) charge in series. The diodes D1 and Do are reverse-biased, and D2 and D3 are forward-biased, as demonstrated in "Fig. (2.a)". Both Inductors stored energy while flowing of the current through them grows linearly.
According to the KVL principle, the voltage equation in this mode can be expressed as:

$$VL1 = Vin \quad (2)$$
$$VL2 = Vin + VC1 \quad (3)$$
$$VC2 = Vin \quad (4)$$

it can be obvious from equations "(1)"and "(2)", the inductor L_2 is storage energy large than input voltage as compared with the inductor L_1.

Mode 2: during the switch (S) is turned OFF, the first inductor (L1) and capacitor (C1) are parallel discharged. In contrast, the capacitor (C2) and inductor (L2) discharge in series to load. The diodes D1 and Do are forward biased, D2 and D3 are reverse-biased, as depicted in "Fig. (2.b)". The voltage equations of inductors can be demonstrated as follows:

$$VL1 = VC1 \quad (5)$$
$$Vin + VC1 - VL2 + VC2 - VO = 0 \quad (6)$$
$$VL2 = VO - 2\,Vin - VC1 \quad (7)$$

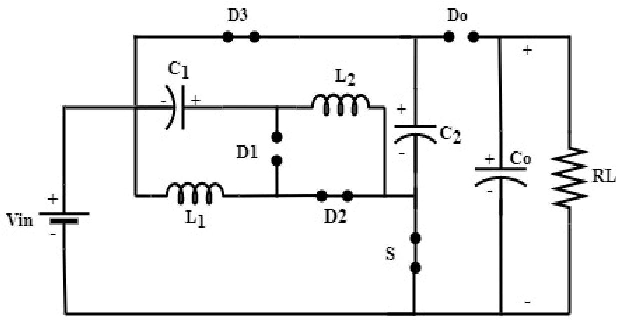

(a)

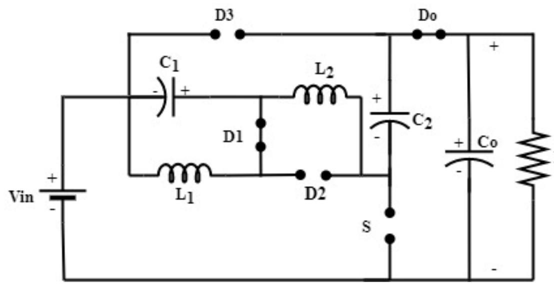

(b)

Fig. 2. The Equivalent Circuit of the proposed new converter at (a) Switch - ON, (b) Switch - OFF

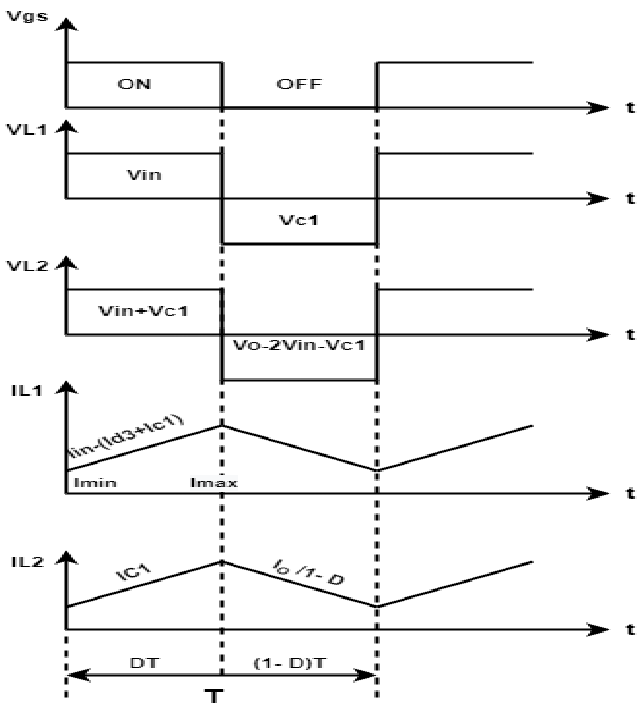

Fig .3. Characteristics of the waveform in CCM

The steady-state of inductors L1 and L2 is calculated by using the voltage second law, the voltage across capacitor C1 can be written as functions of duty cycle and input voltage after substitute equations" (2)" and "(5)", we get:

$$VL_1 T_{ON} = VL_1 T_{OFF} \quad (8)$$

Where , $T_{ON} = DT$ and $T_{OFF} = (1 - D)T$

$$V_{C1} = \frac{D\,V_{in}}{1-D} \quad (9)$$
$$VL_2 T_{ON} = VL_2 T_{OFF} \quad (10)$$

To extract the final gain ratio of the proposed converter, the equations "(3)", "(7)", and "(9)" are substituted in "equation (10)", and we get:

$$(V_{in} + V_{C1})\,DT = (V_O - 2V_{in} - V_{C1})\,(1 - D)\,T \quad (11)$$

As a result, the relationship for the voltage transfer ratio can be expressed:

$$\text{Gain ratio is } \; G = \frac{V_O}{Vin} = \frac{(1-D)^2+1}{(1-D)^2} \quad (12)$$

The output voltage would be as follows:

$$V_O = \frac{(1-D)^2+1}{(1-D)^2} V_{in} \tag{13}$$

From "equation (13)", the voltage gain for our converter is quadratic. To show the step-up ratio against the duty cycle and compare it with the traditional boost converter described in "equation (1)", "Fig. 4" demonstrates that the proposed converter is outstanding in step-up input for multi-times of inputs. From this Figure, the proposed converter's behavior is quadratic and jumps considerably with each varied value of the duty cycle.

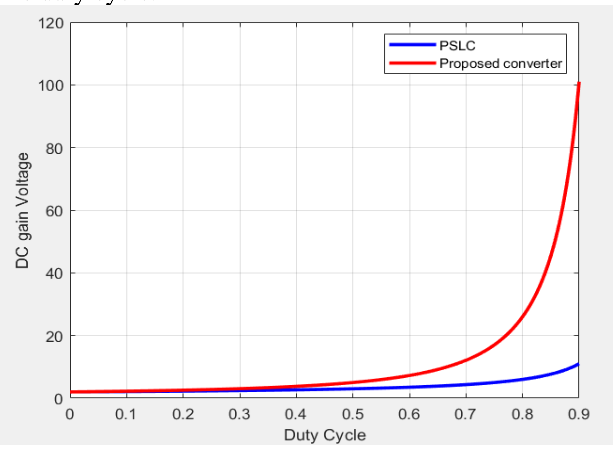

Fig. 4. The voltage gains ratio (G) of the elementary (POSL) converter and the proposed converter are Compared.

B. Current equations

During ON switch

$$I_O = I_{CO} \tag{14}$$

$$I_{C1} = I_{L2} \tag{15}$$

With ideal passive elements (no losses), we conclude:

$$P_{in} = P_o \tag{16}$$

$$I_{in} V_{in} = I_O V_O \tag{17}$$

As a result, the input current can be written as:

$$\frac{I_{in}}{I_O} = \frac{V_O}{V_{in}} = \frac{(1-D)^2+1}{(1-D)^2} \tag{18}$$

$$I_{in} = \frac{(1-D)^2+1}{(1-D)^2} \times I_O \tag{19}$$

Where I_O is the output current passing through the resistive. According to the balance charge principle in a steady-state $Q_{CO+} = Q_{CO-}$ and we can be defined the charge during off and on the state as:

$$Q_{CO+} = I_O DT \tag{20}$$

$$Q_{CO-} = I_{CO}(1-D)T \tag{21}$$

As a result of equations "(20)" and "(21)", we get the following:

$$Ico_{OFF} = \frac{D}{1-D} I_O \tag{22}$$

$$Ido_{OFF} = Ico_{OFF} + I_O \tag{23}$$

$$Ido_{OFF} = \frac{1}{1-D} I_O \tag{24}$$

$$I_{L2} = I_{C2} = Ido_{OFF} = \frac{I_O}{1-D} \tag{25}$$

Also, for capacitor C_1

$$Q_{C1+} = Q_{C1-}$$

$$I_{C1-on} = \frac{1-D}{D} \times \frac{I_o}{1-D} = \frac{I_o}{D} \tag{26}$$

$$I_{C1-OFF} = I_{L2} - I_{L1} \tag{27}$$

Where

$$I_{L1} = \frac{D\, I_o}{(1-D)^2} \tag{28}$$

$$I_{C1-OFF} = \frac{I_o}{(1-D)} - D\,\frac{I_o}{(1-D)^2} \tag{29}$$

As a result, the capacitor current during the off-state is:

$$I_{C1-OFF} = \frac{1-2D}{(1-D)^2} I_O \tag{30}$$

C. Voltage stress across switches

The voltage stress across diodes and the MOSFET switch are given by equations "(31)" to "(44)".

During the ON switch, the output diode can be defined by the equations as:

$$V_{in} - V_{do} - V_O = 0 \tag{31}$$

$$V_{do} = -(V_O - V_{in}) \tag{32}$$

During the OFF switch, the voltage stress across D3 is:

$$V_{in} - V_{d3} - V_O = 0 \tag{33}$$

$$V_{d3} = -(V_O - V_{in}) = V_{do} \tag{34}$$

Also, the voltage stress across the D1 during the ON switch is:

$$V_{in} + V_{C1} + V_{d1} = 0 \tag{35}$$

$$V_{d1} = -(V_{in} + V_{C1}) \tag{36}$$

$$V_{d1} = \frac{-V_{in}}{1-D} \tag{37}$$

According to the KVL law, the voltage stress across the MOSFET switch and D2 during the OFF switch are:

$$V_S + V_{C2} + V_O = 0 \tag{38}$$

$$V_S = V_O - V_{C2} \tag{39}$$

$$V_S = V_O - V_{in} \tag{40}$$

$$V_{in} + V_{L1} - V_{d2} - V_S = 0 \tag{41}$$

$$V_{d2} = V_{in} + V_{L1} - V_S \tag{42}$$

$$V_{d2} = \frac{2-D}{1-D} V_{in} - V_O \tag{43}$$

$$V_{d2} = \frac{D}{(1-D)^2} V_{in} \tag{44}$$

D. Design of passive elements:

1) Inductors L1, L2

When the first mode of operation's equation is re-written in differential form, the driven design equation of the inductor can be described in the following equations:

$$V_{in} = V_{L1} = L_1 \frac{\Delta i L_1}{\Delta t} \tag{45}$$

$$L_1 = \frac{V_{in}\Delta t}{\Delta i L_1} \tag{46}$$

$$L_1 = \frac{V_{in} D}{F_S\, \Delta i L_1} \tag{47}$$

Similarly, for L2, during the OFF switch, we get:

$$V_{L2} = V_{in} + V_{C1} \tag{48}$$

$$= V_{in} + \frac{D}{1-D} V_{in} \tag{49}$$

$$= V_{in}\left(1 + \frac{D}{1-D}\right) \tag{50}$$

$$= \frac{1}{1-D} V_{in} \rightarrow V_{L2} = \frac{V_{in}}{1-D} = L_2 \frac{\Delta i\, L_2}{\Delta t} \tag{51}$$

$$L_2 = \frac{V_{in}\, D}{F_S\, \Delta i L_2 (1-D)} \tag{52}$$

2) Design of capacitors (C_1, C_2, C_O)

To operate the proposed converter, it should design the capacitor value according to the minimal permitted ripple. The output capacitor C_O can be designed according to the storage energy principle ($\Delta Q = C\Delta V_O$, $\Delta Q = I_O DT$, $\Delta Q = \frac{V_O D}{R\,F_s}$) as:

$$C\Delta V_O = \frac{V_O D}{R\,F_s} \tag{53}$$

$$C_O = \frac{V_O D}{R\,F_s\,\Delta V_O} \tag{54}$$

According to the relationship of current and voltage across of capacitor, the value of capacitor C_1 can be calculated as:

$$i_{C1} = C_1 \frac{\Delta V_{C1}}{\Delta t} \rightarrow C_1 = \frac{i_{C1}\Delta t}{\Delta VC_1} \tag{55}$$

$$C_1 = \frac{V_O(1-2D)}{RF_s\,\Delta V_{C1}(1-D)} \text{ OR } C_1 = \frac{(1-D)(1-2D)}{F_s\,\Delta V_{C1}((1-D)^2+1)} \tag{56}$$

Similarly, for Capacitor C_2, we get:

$$i_{C2} = C_2 \frac{\Delta V_{C2}}{\Delta t} \rightarrow C_2 = \frac{i_{C2}\Delta t}{\Delta VC_2} \tag{57}$$

$$C_2 = \frac{I_{in}(1-D)^2}{((1-D)^2+1)F_s\,\Delta V_{C2}} \tag{58}$$

III. CONTROL STRATEGY

The PI controller represents one of the commonly used control methods for the DC-DC converters, which is used in many industrial fields. The PI controller is the best choice for a converter that may be used as a band filter [16]. The control signal from the PI controller is based on the error function as in "equation (59)".

$$u(t) = K_P\, e(t) + \int_0^t K_i\, e(t)dt \tag{59}$$

"Fig. 5" depicts the converter with a PI controller's general block diagram. The error signal is fed into the PI controller to generate the switching signal.

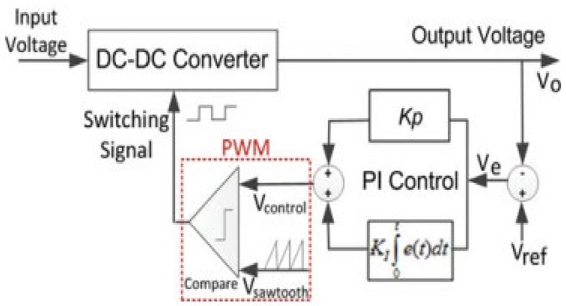

Fig.5. PWM DC-DC Controller based on PI controller [16].

IV. COMPARISON RESULTS

The suggested converter compares with the converters mentioned in this section. The proposed converter is a DC-DC high step-up converter derived from a (POSL) converter. A proposed converter has been compared with other adapters, it has been shown in Table 1. The taken specifications for the comparison are mentioned in Table 1. As displayed, the derived topology has a small number of components, also it is distinguished by a single switch and a simple circuit, which increases reliability and reduces the cost of the proposed converter [17-25].

TABLE 1. Components comparison between the new proposed converter with other converters

Converter Topology	**No. of Components**					**Voltage gain in CCM**
	Switch	***inductor***	***capacitor***	***Diode***	***Total***	
Presented in [17]	2	3	3	4	12	$\frac{2}{D(1-D)}$
Presented in [18]	2	2	2	4	10	$\frac{(1+D)}{D(1-D)}$
Presented in [19]	2	2	2	3	9	$\frac{1}{D(1-D)}$
Presented in [20]	1	2	4	5	12	$\frac{1}{3(1-D)}$
Presented in [21]	1	2	2	3	8	$\frac{2}{(1-D)}$
Presented in [22]	2	3	5	4	14	$\frac{(2-D)(1+D)}{D^2}$
Presented in [23]	1	2	3	4	10	$\frac{(3-D)}{(1-D)}$
Presented in [24]	1	4	5	4	14	$\frac{2D}{(1-D)^2}$
Presented in [25]	1	2	4	5	12	$\frac{2}{(1-D)^2}$
Proposed Converter	1	2	3	4	10	$\frac{(1-D)^2+1}{(1-D)^2}$

V. SIMULATION AND EXPERIMENTAL RESULTS

To prove our theoretical analysis of the proposed converter and comparison the results related to the elementary converter, a new prototype has been established, the performance of the elemental converter and comparison with our converter which is implemented in MATLAB/SIMULINK. Whereby testing of hardware prototypes which are displayed in "Fig. 8". Moreover, the proposed converter test parameters are designed according to the above equations. The design component value as shown in Table (2). The proposed converter designed for dc applications that are based on solar PV. To evaluate the converter performance through the simulation and experiment, the duty ratio as maintained would be 0.5 and the applied voltage is 18.5 V for those two converters. The output voltage has approximately value of (55.5) V for the elementary converter which would be (92) V for the proposed converter. Each device consists of a converter, ARDUINO controller, voltage source, and a load. The converter frequency is 50 kHz. The proposed converter operated at CCM. In order to control the voltage and the current for the proposed converter across the power MOSFET we used ARDUINO microcontroller. The simulation results for the elementary and the proposed converter have been displayed in the "Fig. 6" and "Fig. 7" respectively. "Fig. 8" presents the practical implementation Hardware prototype of the (POSL) converter elementary and proposed converter circuit. The figures from "(9)" to "(10)" displayed the comparison between the practical and experimental with related to the following properties input and output voltages, duty cycle waves, the voltage across inductors and each diode. We also notice in "Fig. 10" that the experimental results of each element of the new proposed converter have fulfilled the above equations and that the output voltage is identical to the "equation (13)". The following table (3) shows the comparison between the theoretical, simulation, and practical work.

TABLE 2. Design value of parameters

Parameter	Value
Input voltage (Vin)	18.5 V
Output voltage (Vo)	92 V
Maximum output power (Po)	150 W
Switching frequency (fs)	50 kHz
Duty cycle (D)	0.5
capacitors C_1=C_2=C_O	100 µF ,400 V
Inductors L1= L2	0.67 µH , 5A
Diodes D_1,D_2,D_3,D_0 (RURG 5060)	50 A, 600 V
Switch MOSFET (IRFP 4060)	40A , 600V
TLP 350 drive	1.5A , 30V
Load Resistance	680 Ω

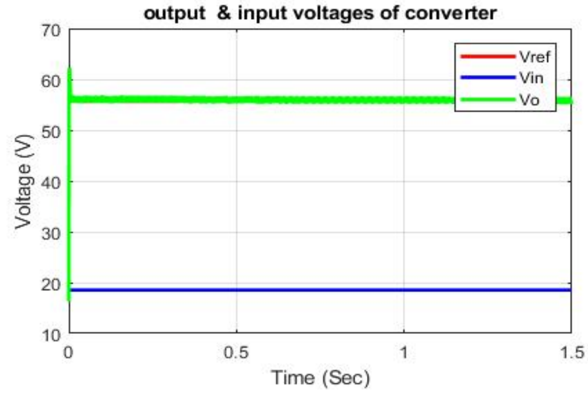

(a)

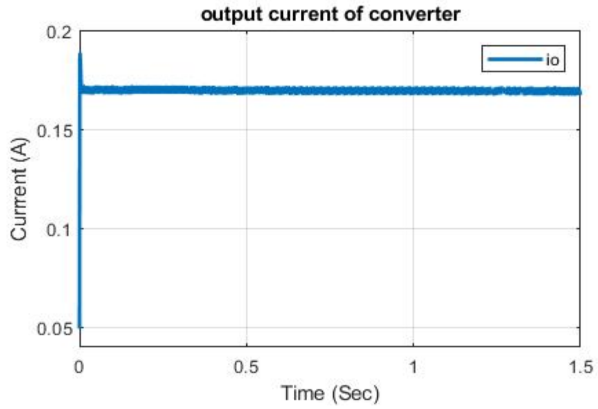

(b)

Fig. 6. Simulation results of elementary (POSL) converter (a) Output and input voltage, (b) Output current

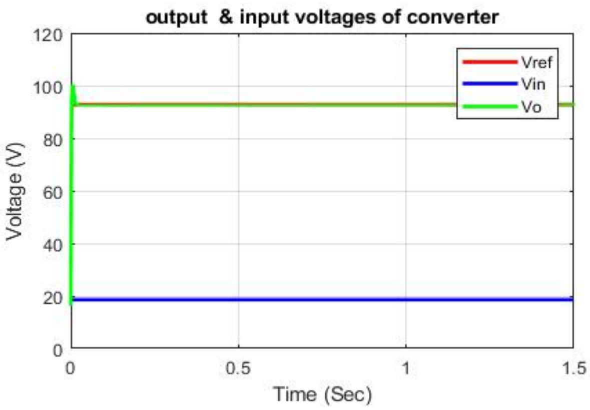

(a)

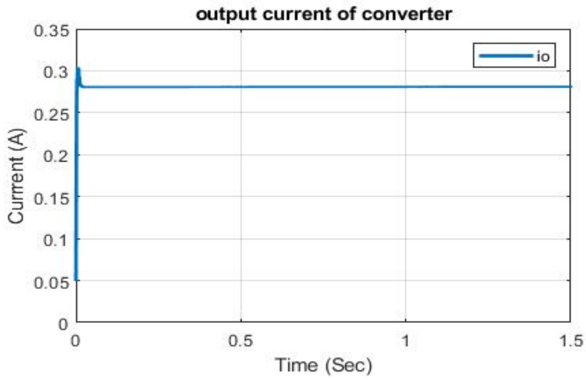

(b)

Fig.7. Simulation results of proposed new converter (a) Output and input voltage, (b) Output current.

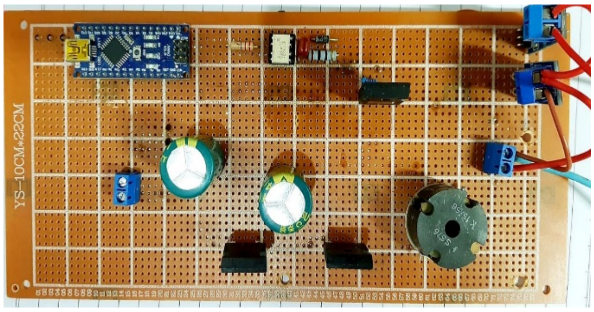

(a)

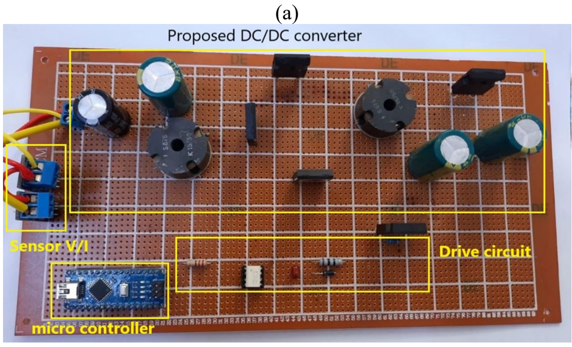

(b)

Fig. 8. Hardware prototype of (a) Elementary (POSL) converter, (b) Proposed new converter.

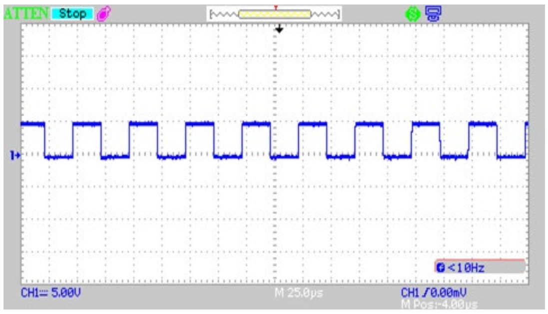

(a) Duty cycle

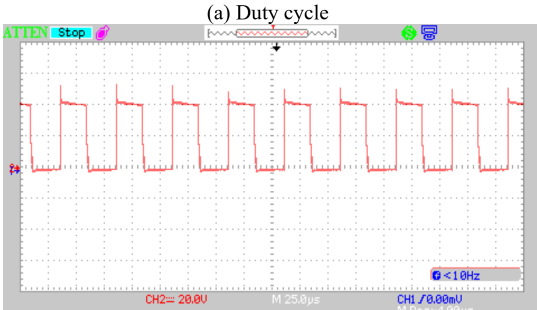

(b) Voltage stress across active switch

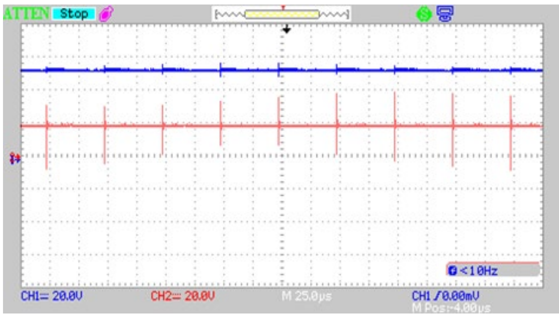

(c) Input & output voltage

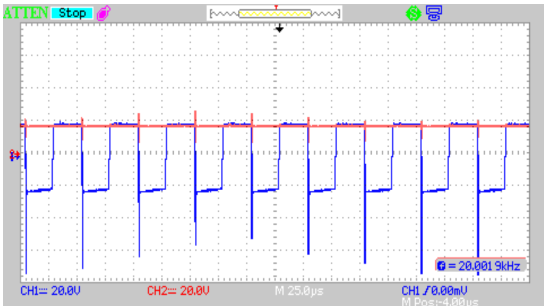

(d) Voltage across inductor and capacitor

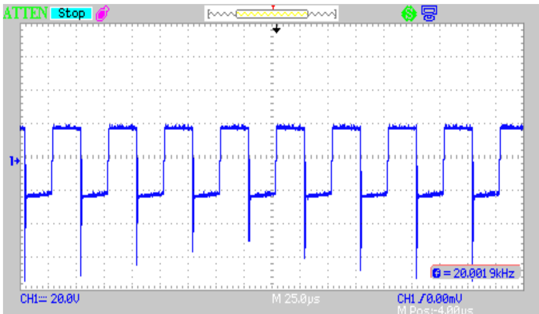

(e) Voltage across the inductor (L1)

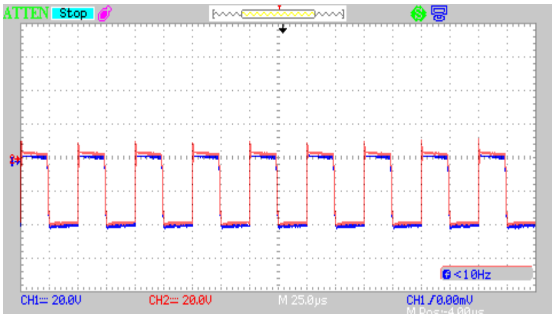

(f) Voltage across diodes (D0 & D1)

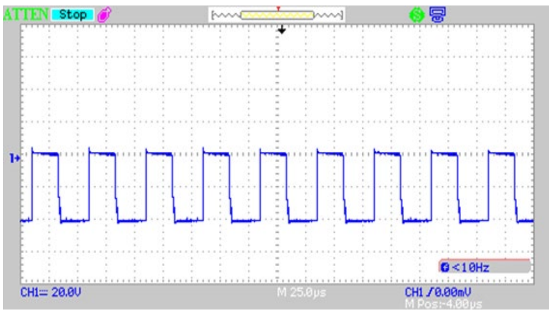

(g) Voltage across the diode (Do)

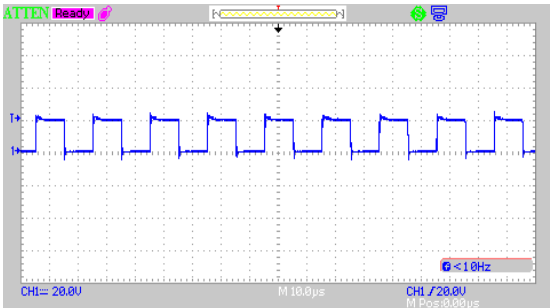

(a) Duty cycle

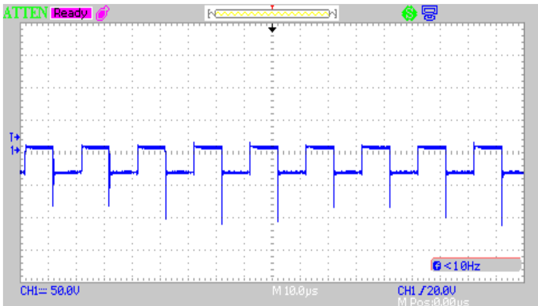

(b) Voltage across the diode (D1)

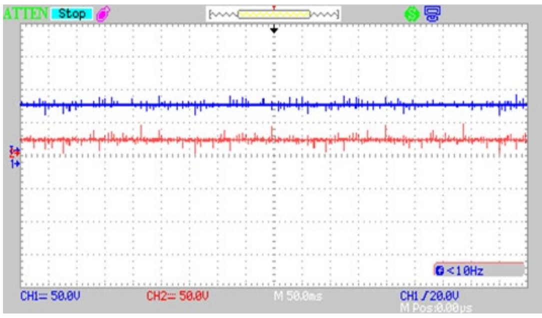

(c) Input & output voltage

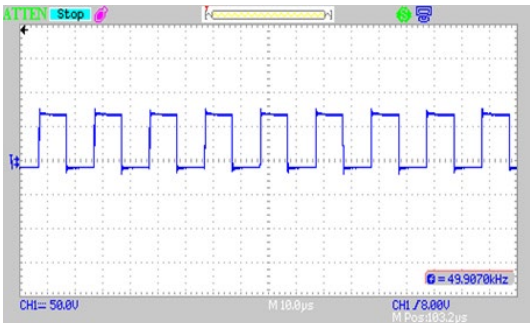

(d) Voltage stress across active switch

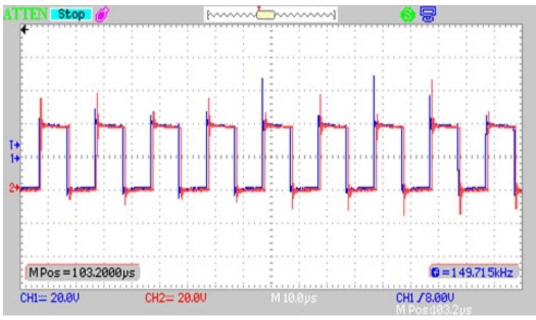

(e) Voltage across inductors (L1 & L2)

Fig. 9. The experimental waves form of elementary (POSL) converter.

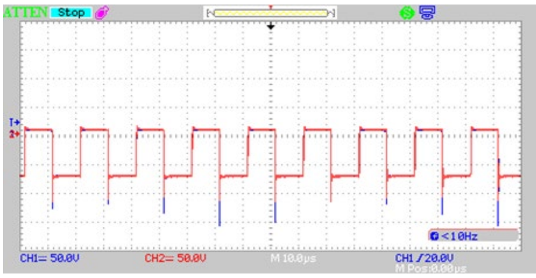

(f) Voltage across diodes (D0 & D3)

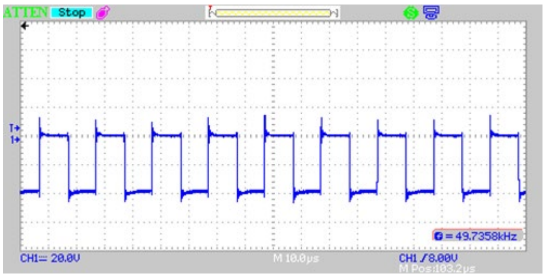

(g) Voltage across the diode (D2)

Fig. 10. The experimental waves form of proposed new converter.

TABLE 3. Experimental results and simulation verification

Parameters	Theoretical results	Simulation results	Hardware results
Output voltage	92.5 V	92.3 V	91.8 V
Output current	0.29 A	0.28 A	0.28 A
Duty cycle	0.5	0.5	0.5

VI. CONCLUSION

Analyzed and proposed a new high-gain converter to achieve significant quadratic voltage gain; the suggested converter only used ten components. Typically, quadratic voltage gain converters use more than one inductor and many diodes. The converter's key characteristic is a constant input current, which extends the lifespan of solar PV panels. In the lab, a 150 W hardware prototype was created. Converter performance and functionality have been proven in experiments. The proposed converter has superior DC gain and switches voltage stress than other high-gain converters like conventional boost and traditional Luo converter. For Vin = 18.5 V, the converter's peak efficiency was 97.3 %. In order to improve our proposed converter performance, we can use other control techniques that are extending another work based on [26-30].

REFERENCES

[1] M. J. Hasan, "Modeling and simulation of 1kw single phase grid tied inverter for solar photovoltaic system," in *IOP Conference Series: Materials Science and Engineering*, 2020, vol. 881, no. 1: IOP Publishing, p. 012139.

[2] M. Luthfansyah, S. Suyanto, and A. B. M. Bangura, "Evaluation and comparison of DC-DC power converter variations in solar panel systems using maximum power point tracking (MPPT) flower pollination algorithm (FPA) Control," in *E3S Web of Conferences*, 2020, vol. 190: EDP Sciences, p. 00026.

[3] K. S. Rathore, U. K. Kalla, D. K. Palwalia, and B. J. I. T. o. E. E. S. Singh, "An improved power quality modified DC‐DC converter fed PMBLDC motor drive system for household applications," vol. 31, no. 10, p. e12620, 2021.

[4] H. K. Khalil, S. S. Hreshee, and H. J. Motlak, "Design and Implementation of Photovoltaic System Based on Super-Lift LUO Converter," in *Journal of Physics: Conference Series*, 2020, vol. 1530, no. 1: IOP Publishing, p. 012013.

[5] S. Dheeban, N. M. Selvan, and L. J. M. T. P. Krishnaveni, "Performance improvement of Photo-Voltaic panels by Super-Lift Luo converter in standalone application," vol. 37, pp. 1163-1171, 2021.

[6] S. J. I. J. o. P. El-Ghanam, "Design, implementation and performance analysis of positive super-lift Luo-converter based on different MOSFET types," vol. 94, no. 6, pp. 833-839, 2020.

[7] L. S. J. I. J. o. C. T. Yang and Applications, "Implementation of high step‐up DC‐DC converter using voltage‐lift and coupled inductor techniques," vol. 46, no. 11, pp. 2079-2097, 2018.

[8] Y. Liu, J. Wang, and H. J. E. Tu, "Design and implementation of finite time nonsingular fast terminal sliding mode control for a novel high step-up DC-DC converter," vol. 12, no. 9, p. 1716, 2019.

[9] K. J. Reddy and N. J. I. A. Sudhakar, "High voltage gain interleaved boost converter with neural network based MPPT controller for fuel cell based electric vehicle applications," vol. 6, pp. 3899-3908, 2018.

[10] S. Saravanan, N. J. J. o. a. r. Ramesh Babu, and technology, "A modified high step-up non-isolated DC-DC converter for PV application," vol. 15, no. 3, pp. 242-249, 2017.

[11] T. Rahimi, L. Ding, H. Gholizadeh, R. S. Shahrivar, and R. J. I. A. Faraji, "An Ultra High Step-Up DC–DC Converter Based on the Boost, Luo, and Voltage Doubler Structure: Mathematical Expression, Simulation, and Experimental," vol. 9, pp. 132011-132024, 2021.

[12] S. Padmanaban, M. S. Bhaskar, P. K. Maroti, F. Blaabjerg, and V. J. E. Fedák, "An original transformer and switched-capacitor (T & SC)-based extension for DC-DC boost converter for high-voltage/low-current renewable energy applications: Hardware implementation of a new T & SC boost converter," vol. 11, no. 4, p. 783, 2018.

[13] T. Shanthi, S. Prabha, and K. J. I. T. o. E. C. Sundaramoorthy, "Non-isolated n-stage high step-up DC-DC converter for low voltage DC source integration," vol. 36, no. 3, pp. 1625-1634, 2021.

[14] V. F. Pires, A. Cordeiro, D. Foito, and J. F. J. I. T. o. V. T. Silva, "High step-up DC–DC converter for fuel cell vehicles based on merged quadratic boost–Ćuk," vol. 68, no. 8, pp. 7521-7530, 2019.

[15] S. Hasanpour, Y. Siwakoti, and F. J. I. P. E. Blaabjerg, "New Single-Switch quadratic boost DC/DC converter with Low voltage stress for renewable energy applications," 2020.

[16] M. E. Şahin, H. İ. J. E. P. C. Okumuş, and Systems, "Comparison of different controllers and stability analysis for photovoltaic powered buck-boost DC-DC converter," vol. 46, no. 2, pp. 149-161, 2018.

[17] F. Mohammadzadeh Shahir, E. Babaei, M. Sabahi, and S. J. I. T. o. E. E. S. Laali, "A new DC‐DC converter based on voltage‐lift technique," vol. 26, no. 6, pp. 1260-1286, 2016.

[18] F. M. Shahir, E. Babaei, and M. J. I. P. E. Farsadi, "Analysis and design of voltage-lift technique-based non-isolated boost dc–dc converter," vol. 11, no. 6, pp. 1083-1091, 2018.

[19] F. M. Shahir, E. Babaei, and M. J. I. T. o. P. E. Farsadi, "Extended topology for a boost DC–DC converter," vol. 34, no. 3, pp. 2375-2384, 2018.

[20] N. Tewari and V. J. S. E. Sreedevi, "A novel single switch dc-dc converter with high voltage gain capability for solar PV based power generation systems," vol. 171, pp. 466-477, 2018.

[21] S. A. Nath and J. Pradeep, "PV based design of improved positive output super-lift Luo converter," in *2016 Second International Conference on Science Technology Engineering and Management (ICONSTEM)*, 2016: IEEE, pp. 293-297.

[22] J. D. Navamani, A. Geetha, D. Almakhles, A. Lavanya, and J. S. M. J. I. A. Ali, "Modified LUO High Gain DC-DC Converter With Minimal Capacitor Stress for Electric Vehicle Application," vol. 9, pp. 122335-122350, 2021.

[23] A. T. Mohammed and N. K. Alshamaa, "Design and Implementation of a Modified Luo Converter with Higher–Voltage Ratio Gain," in *IOP Conference Series: Materials Science and Engineering*, 2020, vol. 881, no. 1: IOP Publishing, p. 012124.

[24] D. J. J. E. d. S. A. Murali, "Steady State Behavior of a Single-Switch Non-isolated DC-DC SEPIC Converter Topology with Improved Static Voltage Gain," vol. 54, no. 3, pp. 445-452, 2021.
[25] A. Nakpin and S. J. P. C. S. Khwan-on, "A novel high step-up DC-DC converter for photovoltaic applications," vol. 86, pp. 409-412, 2016.
[26] C. H. KOM and B. M. LONLA, "Duty Cycle Modulation and Fuzzy Controller of a Chopper Extracting the Maximum Power Point of a Solar Panel," *International Journal of Renewable Energy Research (IJRER),* vol. 12, no. 1, pp. 70-80, 2022.
[27] Y. Palleswari, "A Novel Hybrid High Gain DC-DC converter for Renewable Energy Applications," *International Journal of Renewable Energy Research (IJRER),* vol. 12, no. 1, pp. 88-96, 2022.
[28] P. Suresh, S. G. Fernandez, and P. Murali, "Design and Implementation of a Novel Zeta Converter for DC Bus Voltage Regulation," *International Journal of Renewable Energy Research (IJRER),* vol. 12, no. 1, pp. 601-610, 2022.
[29] V. H. Avila and V. Leite, "Control of grid-connected inverter output current: A practical review," in *2020 9th International Conference on Renewable Energy Research and Application (ICRERA)*, 2020: IEEE, pp. 232-235.
[30] A. Belkaid, I. COLAK, K. KAYISLI, and R. BAYINDIR, "Improving PV system performance using high efficiency fuzzy logic control," in *2020 8th International Conference on Smart Grid (icSmartGrid)*, 2020: IEEE, pp. 152-156.

BIOGRAPHIES OF AUTHORS :-

	Zainab A. Ghafour has attained her B.Sc. from the Department of Electrical Power/ Technical College / Al Mussaib (TCM)/ Al Furat Al Awsat Technical University. She is now M.Sc. student in Electrical Power Department in the research phase / Electrical Engineering Technical College/ Middle Technical University since October 2020, Baghdad, Iraq.
	Assist. Prof. Dr. Ahmed R. Ajel, was born in Iraq Baghdad. He received his BSc., M.Sc. and PhD. In Electrical and Electronics Engineering in 1992, 1997, and 2006 respectively at the university of technology. So there are these links related to him: https://scholar.google.com/citations?user=lGnNxJMAAAAJ&hl=en https://www.researchgate.net/profile/Ahmed-R
	Assist. Prof Dr. Naseer M. Yasin is a lecturer at the Electrical Engineering Technical College/Middle Technical University, Baghdad, Iraq. He received the BSc. Degree in electric engineering / Royal military college, UK, Sweden, MSc. Degree in power engineering / Electric Engineering Technical college and received his Ph.D. degree in power and Machines engineering / Basra University in 1989, 2007, and 2014 respectively.